

Microstructure, Toughness and Hardness of the Simulated HAZ Area of Steel S1300QL

Abstract: The introduction contains information (found in available reference publications) concerning the weldability of steel S1300QL. The introduction also presents general information concerning the effect of the microstructure and the chemical composition of filler metals used in the welding of high-strength steels on the mechanical properties of weld deposit. The subject of simulation tests (discussed in the article) was structural steel S1300QL having a yield point of more than 900 MPa S1300QL. Simulations involved both single ($T_{\max} = 1250^{\circ}\text{C}$) and double welding thermal cycles ($T_{\max} = 1250^{\circ}\text{C} + 600^{\circ}\text{C}$, $T_{\max} = 1250^{\circ}\text{C} + 760^{\circ}\text{C}$ and $T_{\max} = 1250^{\circ}\text{C} + 900^{\circ}\text{C}$) as well as cooling times $t_{8/5} = 3$ s, 5 s and 10 s. Specimens with simulated HAZ areas were subjected to impact strength tests performed at a temperature of -40°C and $+20^{\circ}\text{C}$, Vickers hardness tests (HV10) and microscopic metallographic tests involving the use of light microscopy. The test results are presented in related diagrams and photographs. The final part of the article contains a discussion concerning test results and concluding remarks. The tests revealed that, in terms of the test steel, the number of repetitions of thermal cycles having pre-set parameters did not explicitly translated into changes of impact energy values concerning the simulated HAZ areas. The tests also revealed that recommended thermal cycles making it possible to obtain the required combination of the high toughness and hardness of the simulated HAZ area of steel S1300QL (similar to that of the base material) were double thermal cycles of maximum temperature $T_{\max 1} = 1250^{\circ}\text{C} + T_{\max 2} = 600^{\circ}\text{C}$ and $T_{\max 1} = 1250^{\circ}\text{C} + T_{\max 2} = 900^{\circ}\text{C}$ combined with cooling times $t_{8/5} = 5$ s and 10 s and all numbers of repeated thermal cycles.

Keywords: Steel S1300QL, weldability of steel, simulation tests

DOI: [10.17729/ebis.2021.6/2](https://doi.org/10.17729/ebis.2021.6/2)

Introduction

High-strength martensitic steels are very attractive structural materials, yet welding such steels poses some problems. A heat input to the joint during the welding process is responsible

for the local deterioration of mechanical properties in the heat affected zone (HAZ).

Modern steels having a yield point exceeding 900 MPa include steel grades manufactured by the SSAB Oxelösund company (Sweden) [1].

Such steels have been designed to satisfy (or even surpass) requirements of an industry producing high-loaded crane structures and other elements. As a result of an advanced metallurgical process, steels S960, S1100 and S1300 are characterised by high metallurgical purity as well as favourable weldability, bendability and machinability [2].

The authors of publication [3] stated that the weldability of steel S1300 is satisfactory, yet it is necessary to take into consideration the risk of cold cracking in over-rigid structures, characterised by the high restraint of elements joined using methods and filler metals having average and high hydrogen contents (above 5 mg/g of weld deposit). Very similar conclusions were drawn by the authors of publication [4].

Because of their specific nature, filler metals used in the welding of high-strength steels should be characterised by a balance between mechanical and plastic properties (primarily toughness) both at low and ambient temperature. However, the analysis of available reference publications revealed that meeting the above-named requirements poses a significant and ongoing challenge. Publication [5] presents test results concerning the positive effect of the weld deposit microstructure (fine-lamellar martensite) on mechanical properties as well as the effect of precipitates such as carbides and/or carbonitrides on plastic properties. The authors of publication [6] stated that weld deposit hardness decreased after the nickel addition increased a certain level, which, in turn, was connected with a manganese content. Various reference publications

discuss the effect of manganese on the properties of weld deposit characterised by a high yield point [6–8].

Presently, in Poland, high-loaded welded structures are made of steels S960 and S1100. Steel grade S1300 is not commonly used because there is no filler metal which could be used in the welding of the aforesaid steel.

This article presents results of simulation tests concerning steel S1300QL, aimed to identify the effect of welding thermal cycles on the microstructure, toughness and hardness of the simulated HAZ area.

Test material

The tests discussed in the article involved the use of 7 mm thick plates made of high-strength steel S1300QL. The analysis of the chemical composition of steel S1300QL was performed using a Q4 TASMANN 170 spark emission spectrometer (Bruker; Germany). The results of the analysis are presented in Table 1.

Testing methodology

Simulation tests

The simulated HAZ area of the test steel was obtained using a Gleeble 3500 thermal-strain cycle simulator (DSI; USA) (Fig. 1). The simulation tests involved the use of impact specimens having dimensions 5 mm × 10 mm × 55 mm.

The simulation required the identification of critical temperatures AC₁ and AC₃ in relation to steel S1300QL. The above-named temperatures were determined using the following equations [9, 10]:

Table 1. Chemical composition of steel S1300QL

Chemical element content, % by weight									
C	Si	Mn	P	S	Cr	Mo	Ni	Cu	B
0.236	0.220	0.855	0.0047	0.0008	0.493	0.401	1.348	0.017	0.0012
Chemical element content, % by weight according to the manufacturer [1]									
C	Si	Mn	P	S	Cr	Mo	Ni	Cu	B
max 0.25	max 0.50	max 1.40	max 0.020	max 0.005	max 0.80	max 0.70	max 3.00	max 0.30	max 0.005

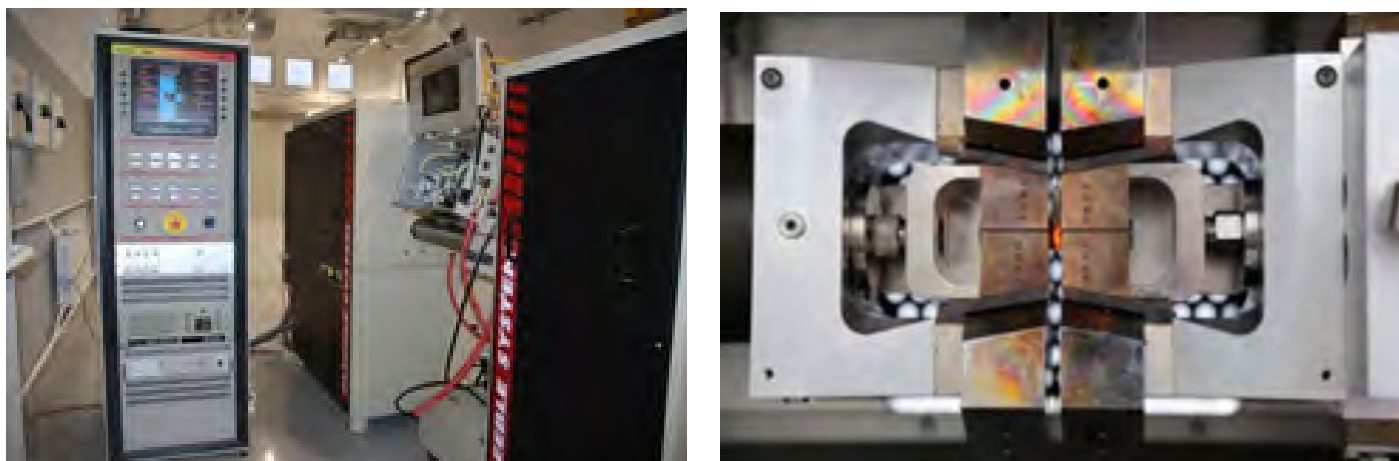


Fig. 1. Gleeble 3500 simulator at Łukasiewicz – Instytut Spawalnictwa: a) main view and b) specimen fixed in the current clamps of the simulator

$$A_{C1} = 723 - 10.7xMn - 16.9xNi + 29.1xSi + 16.9xCr + 290xAs + 6.38xW \quad [1]$$

$$A_{C3} = 910 - 203xC^{1/2} - 15.2xNi + 44.7xSi + 104xV + 31.5xMo + 13.1xW - (30xMn + 11xCr + 20xCu - 700xP - 400xAl - 120xAs - 400xTi) \quad [2]$$

The use of the chemical element contents (presented in Table 1) in equations [1] and [2] enabled the identification of critical temperature values in relation to steel S1300QL, i.e. $A_{C1} = 706^{\circ}\text{C}$ and $A_{C3} = 814^{\circ}\text{C}$.

The idea of the programme, presented in Table 2, was to simulate thermal conditions during the actual MAG welding of steel S1300QL involving the single and double effect of the welding thermal cycle.

Impact strength tests

After the simulation, 2 mm deep Charpy V type notches were made centrally in the HAZ. The impact tests were performed at a temperature of -40°C and $+20^{\circ}\text{C}$ (in accordance with the requirements of standard PN-EN ISO 148-1 [11])

Table 2. Simulation parameters

Single thermal cycle		
$T_{max}, ^{\circ}\text{C}$	$t_{8/5}, \text{s}$	
1250	3	
	5	
	10	
Double thermal cycle		
$T_{max1}, ^{\circ}\text{C}$	$T_{max2}, ^{\circ}\text{C}$	$t_{8/5}, \text{s}$
1250	600 (below temperature A_{C1})	5
		10
	760 (between A_{C1} and A_{C3})	5
		10
	900 (above temperature A_{C3})	5
		10

Where

- a) T_{max} – maximum temperature of the welding thermal cycle,
- b) $t_{8/5}$ – time of HAZ cooling between 800°C and 500°C ,
- c) A_{C1}, A_{C3} – critical temperatures,
- d) number of thermal cycle repetitions: 1, 2 and 3 times (where 1 – simulation of production welding and 2 and 3 – simulations of the first and second repair welding respectively).

using an Amsler RPK 300 impact testing machine (Germany).

Microscopic metallographic tests of simulated HAZ areas

Metallographic specimens (for microscopic tests) prepared on simulated HAZ areas were subjected to light microscopy-based tests (in accordance with the requirements of the PN-EN ISO 17639 standard) [12]. The microstructure of the specimens was revealed through Nital-based chemical etching. The microscopic tests were performed using a Nikon Eclipse MA 200 optical metallographic inverted microscope (Nikon; Japan) and NIS Elements-AR measurement software (Nikon).

Hardness measurements of simulated HAZ areas

The simulated HAZ areas were subjected to Vickers hardness tests performed using a KB-50BVZ-FA automatic hardness tester (Prüftechnik GmbH; Germany) and a penetrator load of



Fig. 2. Base material of steel S1300QL: martensite, hardness: 486 HV_{10av.}, mag. 500x

98.1 N (HV₁₀) (in accordance with the requirements of the PN-EN ISO 6507-1 standard) [13].

Test results

Microscopic metallographic tests of simulated HAZ areas

The results of the microscopic metallographic tests of the base material of steel S1300QL are presented in Figure 2, whereas the results concerning the simulated HAZ areas of steel S1300QL are presented in Figures 3–11.



Fig. 3. Microstructure of steel S1300QL after simulation involving one thermal cycle in relation to cooling time $t_{8/5} = 3$ s: a) heating 1x, martensite, hardness: 451 HV_{10av.}, mag. 500x, b) heating 2x, martensite, hardness 466 HV_{10av.}, mag. 500x, and c) heating 3x, martensite, hardness 462 HV_{10av.}, mag. 500x





Fig. 5. Microstructure of steel S1300QL after simulation involving one thermal cycle in relation to cooling time $t_{8/5} = 10$ s: a) heating 1x, martensite, hardness: 482 HV $_{10_{av}}$, mag. 500x, b) heating 2x, martensite, hardness 486 HV $_{10_{av}}$, mag. 500x, and c) heating 3x, martensite, hardness 433 HV $_{10_{av}}$, mag. 500x



Fig. 6. Microstructure of steel S1300QL after simulation involving double thermal cycle ($T_{max1} = 1250^{\circ}\text{C} + T_{max2} = 600^{\circ}\text{C}$) in relation to cooling time $t_{8/5} = 5$ s: a) heating 1x, mixture of bainite and martensite, hardness: 344 HV $_{10_{av}}$, mag. 500x, b) heating 2x, mixture of bainite and martensite, hardness: 339 HV $_{10_{av}}$, mag. 500x and c) heating 3x, mixture of bainite and martensite, hardness: 339 HV $_{10_{av}}$, mag. 500x



Fig. 7. Microstructure of steel S1300QL after simulation involving double thermal cycle ($T_{max1} = 1250^{\circ}\text{C} + T_{max2} = 600^{\circ}\text{C}$) in relation to cooling time $t_{8/5} = 10$ s: a) heating 1x, mixture of bainite and martensite, hardness: 348 HV $_{10_{av}}$, mag. 500x, b) heating 2x, mixture of bainite, martensite and small amounts of ferrite, hardness: 349 HV $_{10_{av}}$, mag. 500x and c) heating 3x, mixture of bainite, martensite and small amounts of ferrite, hardness: 363 HV $_{10_{av}}$, mag. 500x

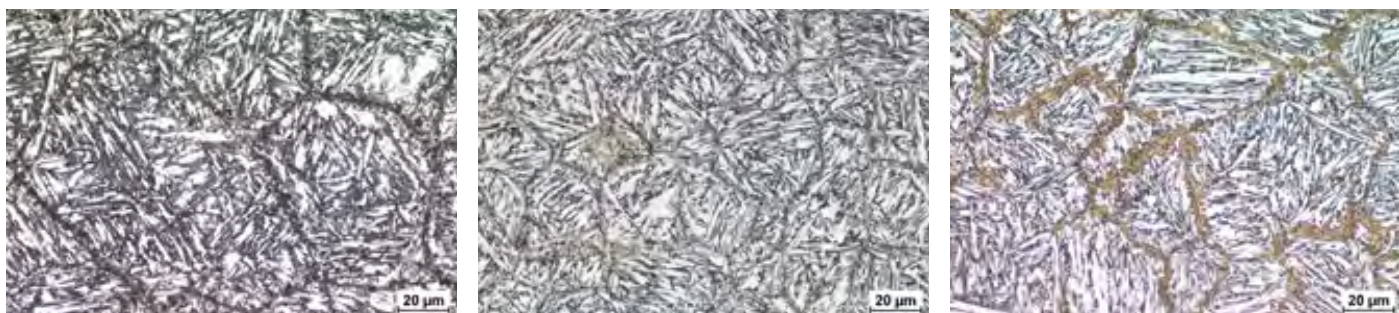


Fig. 8. Microstructure of steel S1300QL after simulation involving double thermal cycle ($T_{max1} = 1250^{\circ}\text{C} + T_{max2} = 760^{\circ}\text{C}$) in relation to cooling time $t_{8/5} = 5$ s: a) heating 1x, mixture of high-tempered martensite and “fresh” martensite along grain boundaries, hardness: 363 HV $_{10_{av}}$, mag. 500x, b) heating 2x, mixture of high-tempered martensite and “fresh” martensite along grain boundaries, hardness: 346 HV $_{10_{av}}$, mag. 500x and c) heating 3x, mixture of high-tempered martensite and “fresh” martensite along grain boundaries, hardness: 360 HV $_{10_{av}}$, mag. 500x

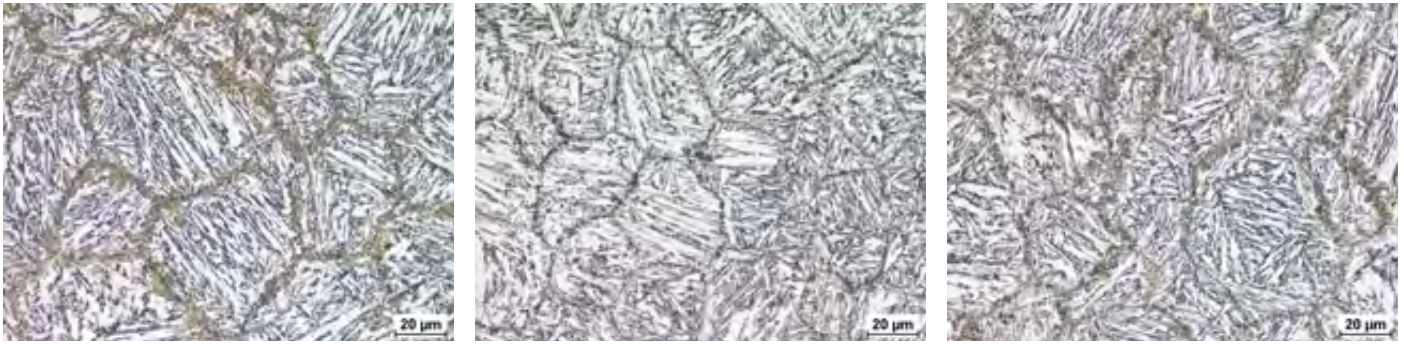


Fig. 9. Microstructure of steel S1300QL after simulation involving double thermal cycle ($T_{max1} = 1250^{\circ}\text{C} + T_{max2} = 760^{\circ}\text{C}$) in relation to cooling time $t_{8/5} = 10$ s: a) heating 1x, mixture of high-tempered martensite and “fresh” martensite along grain boundaries, hardness: 340 HV $_{10_{av}}$, mag. 500x, b) heating 2x, mixture of high-tempered martensite and “fresh” martensite along grain boundaries, hardness: 360 HV $_{10_{av}}$, mag. 500x and c) heating 3x, mixture of high-tempered martensite and “fresh” martensite along grain boundaries, hardness: 347 HV $_{10_{av}}$, mag. 500x



Fig. 10. Microstructure of steel S1300QL after simulation involving double thermal cycle ($T_{max1} = 1250^{\circ}\text{C} + T_{max2} = 900^{\circ}\text{C}$) in relation to cooling time $t_{8/5} = 5$ s: a) heating 1x, martensite and small amounts of ferrite, hardness: 474 HV $_{10_{av}}$, mag. 500x, b) heating 2x, martensite and traces of ferrite, hardness: 483 HV $_{10_{av}}$, mag. 500x and c) heating 3x, martensite and traces of ferrite, hardness: 478 HV $_{10_{av}}$, mag. 500x



Fig. 11. Microstructure of steel S1300QL after simulation involving double thermal cycle ($T_{max1} = 1250^{\circ}\text{C} + T_{max2} = 900^{\circ}\text{C}$) in relation to cooling time $t_{8/5} = 10$ s: a) heating 1x, martensite and traces of ferrite, hardness: 482 HV $_{10_{av}}$, mag. 500x, b) heating 2x, martensite and traces of ferrite, hardness: 462 HV $_{10_{av}}$, mag. 500x and c) heating 3x, martensite and traces of ferrite, hardness: 476 HV $_{10_{av}}$, mag. 500x

Impact strength tests

Impact energy test results concerning all simulation variants and numbers of welding thermal cycles are presented in Figures 12–15.

Measurements of the hardness of simulated HAZ areas

Hardness measurement results concerning all simulation variants and numbers of welding thermal cycles are presented in Figures 16 and 17.

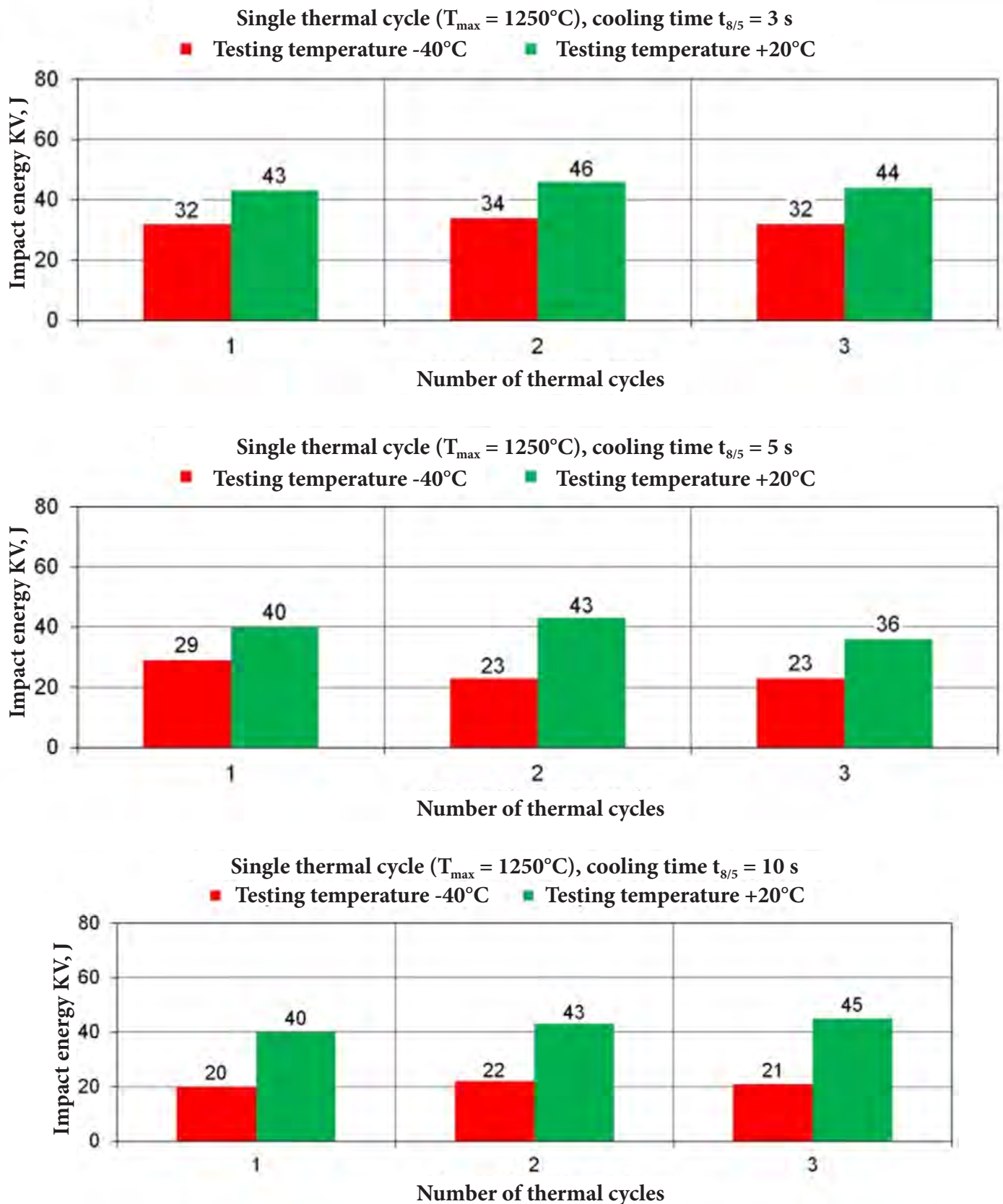
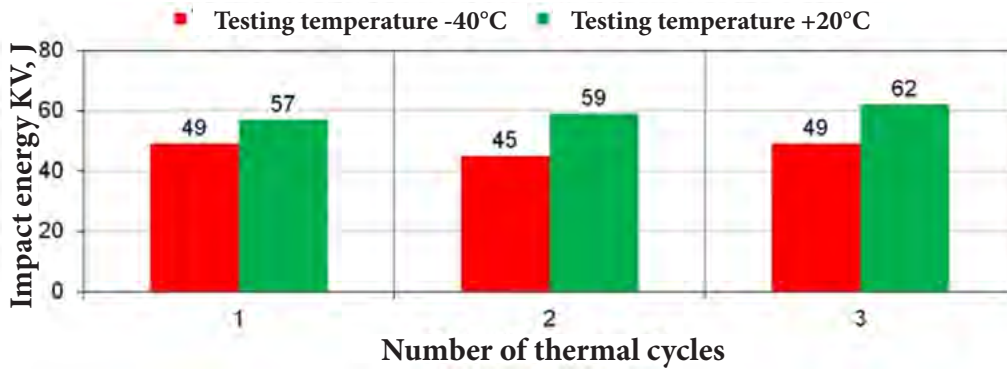


Fig. 12. Impact energy KV of the simulated HAZ areas of steel S1300QL in relation to the single thermal cycle in the function of the number of welding thermal cycles in relation to cooling time $t_{8/5}$: a) 3 s, b) 5 s and c) 10 s

Double thermal cycle ($T_{max1} = 1250^{\circ}\text{C} + T_{max2} = 600^{\circ}\text{C}$, cooling time $t_{8/5} = 5\text{s}$)



Double thermal cycle ($T_{max1} = 1250^{\circ}\text{C} + T_{max2} = 600^{\circ}\text{C}$, cooling time $t_{8/5} = 10\text{s}$)

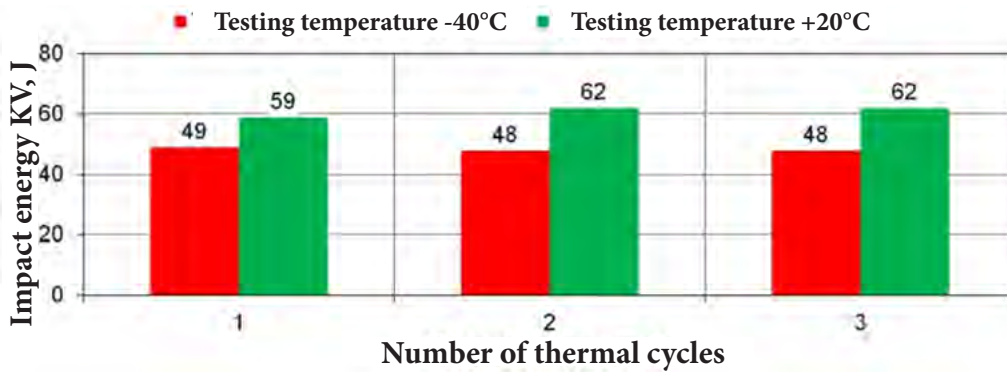
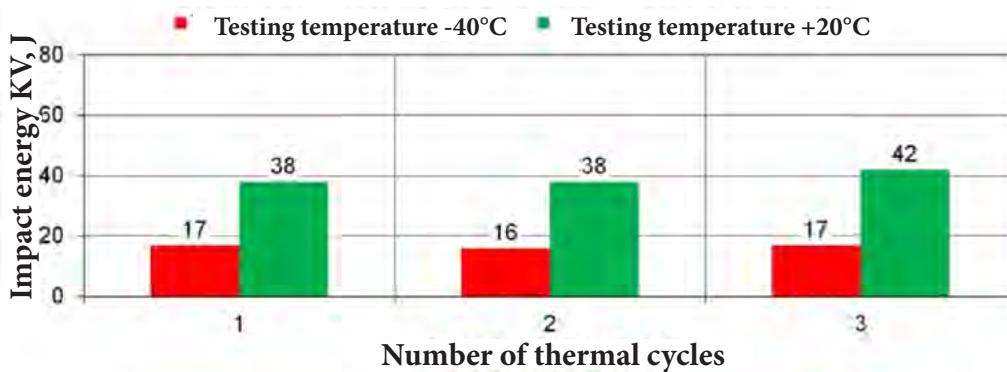


Fig. 13. Impact energy KV of the simulated HAZ areas of steel S1300QL in relation to the double thermal cycle ($T_{max1} = 1250^{\circ}\text{C} + T_{max2} = 600^{\circ}\text{C}$) in the function of the number of welding thermal cycles in relation to cooling time $t_{8/5}$: a) 5 s and b) 10 s

Double thermal cycle ($T_{max1} = 1250^{\circ}\text{C} + T_{max2} = 760^{\circ}\text{C}$, cooling time $t_{8/5} = 5\text{s}$)



Double thermal cycle ($T_{max1} = 1250^{\circ}\text{C} + T_{max2} = 760^{\circ}\text{C}$, cooling time $t_{8/5} = 10\text{s}$)

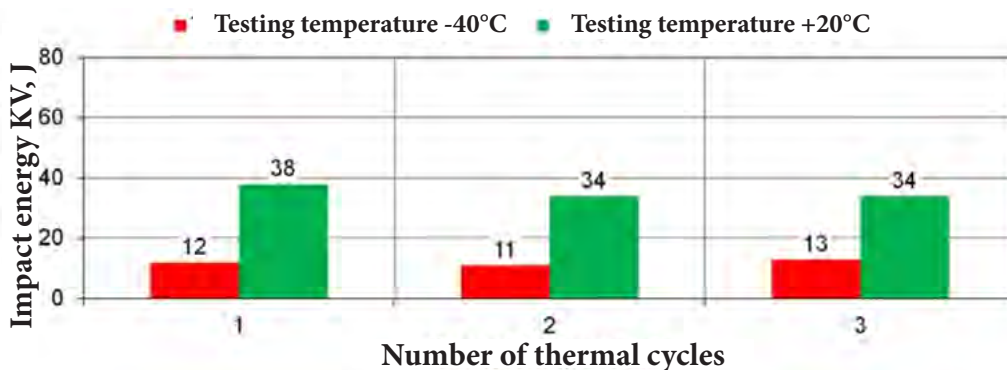
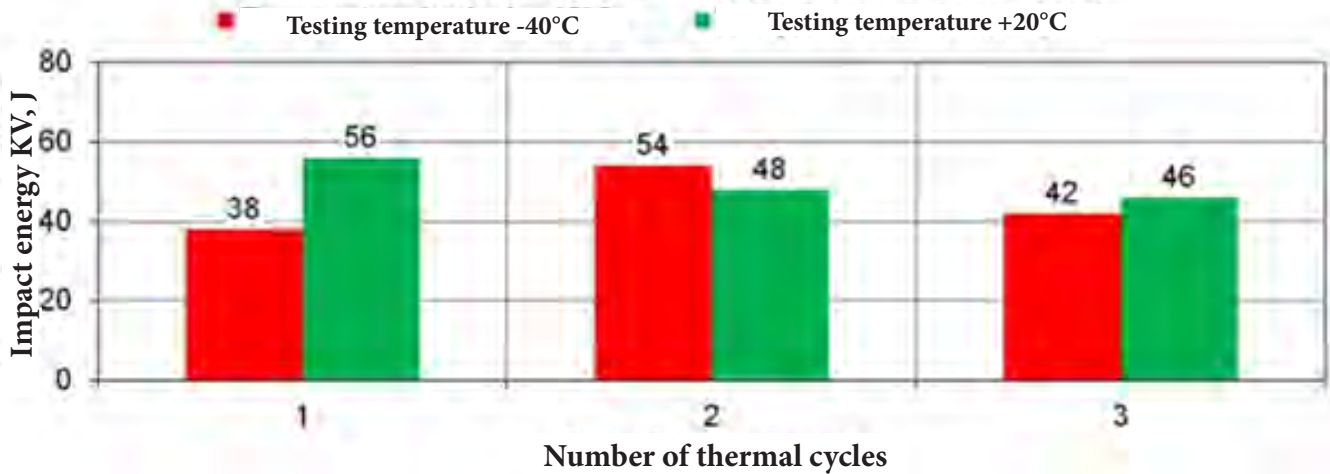


Fig. 14. Impact energy KV of the simulated HAZ areas of steel S1300QL in relation to the double thermal cycle ($T_{max1} = 1250^{\circ}\text{C} + T_{max2} = 760^{\circ}\text{C}$) in the function of the number of welding thermal cycles in relation to cooling time $t_{8/5}$: a) 5 s and b) 10 s

Double thermal cycle ($T_{max1} = 1250^{\circ}\text{C} + T_{max2} = 900^{\circ}\text{C}$, cooling time $t_{8/5} = 5\text{s}$)



Double thermal cycle ($T_{max1} = 1250^{\circ}\text{C} + T_{max2} = 900^{\circ}\text{C}$, cooling time $t_{8/5} = 10\text{s}$)

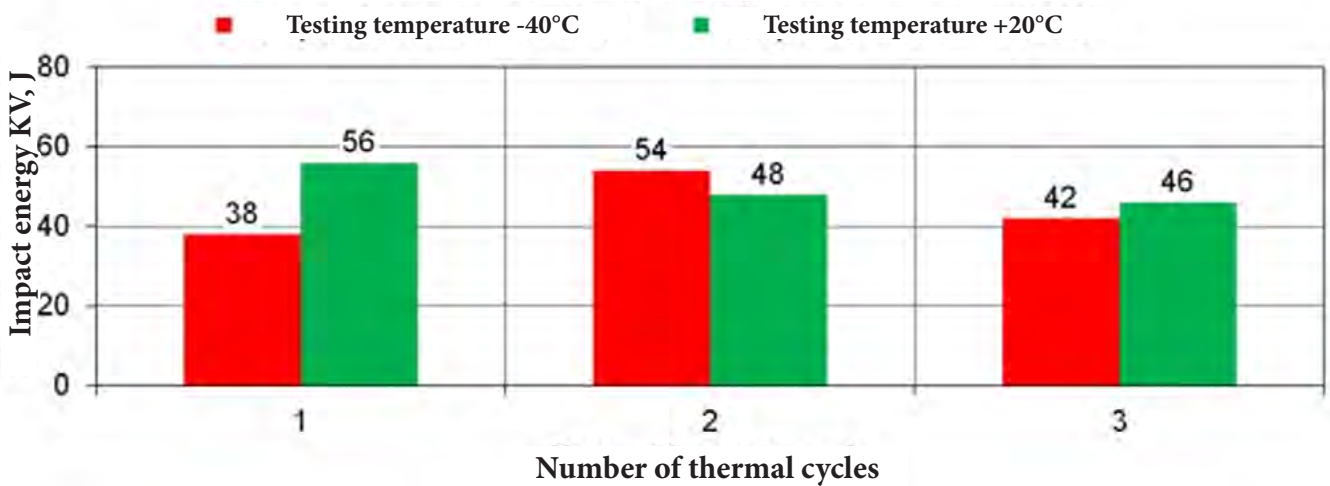


Fig. 15. Impact energy KV of the simulated HAZ areas of steel S1300QL in relation to the double thermal cycle ($T_{max1} = 1250^{\circ}\text{C} + T_{max2} = 900^{\circ}\text{C}$) in the function of the number of welding thermal cycles in relation to cooling time $t_{8/5}$: a) 5 s and b) 10 s

Single thermal cycle ($T_{max} = 1250^{\circ}\text{C}$)

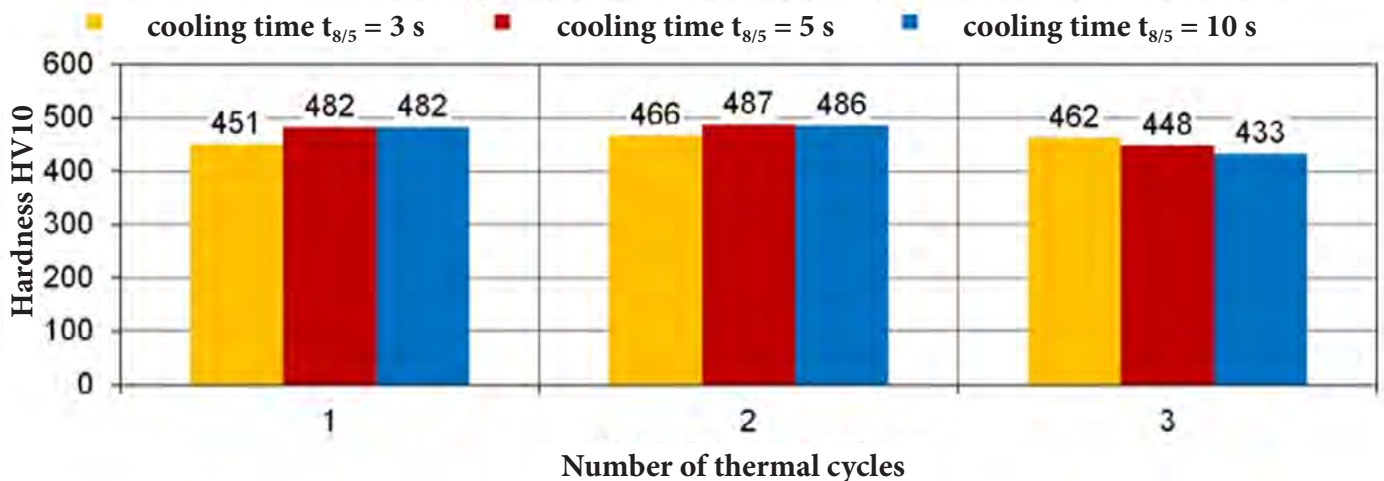


Fig. 16 Average values of hardness HV10 in relation to the simulated SWC areas of steel S1300QL in relation to the single thermal cycle $T_{max} = 1250^{\circ}\text{C}$ in the function of the number of welding thermal cycles in relation to cooling time $t_{8/5} = 3\text{s}$, 5s and 10s

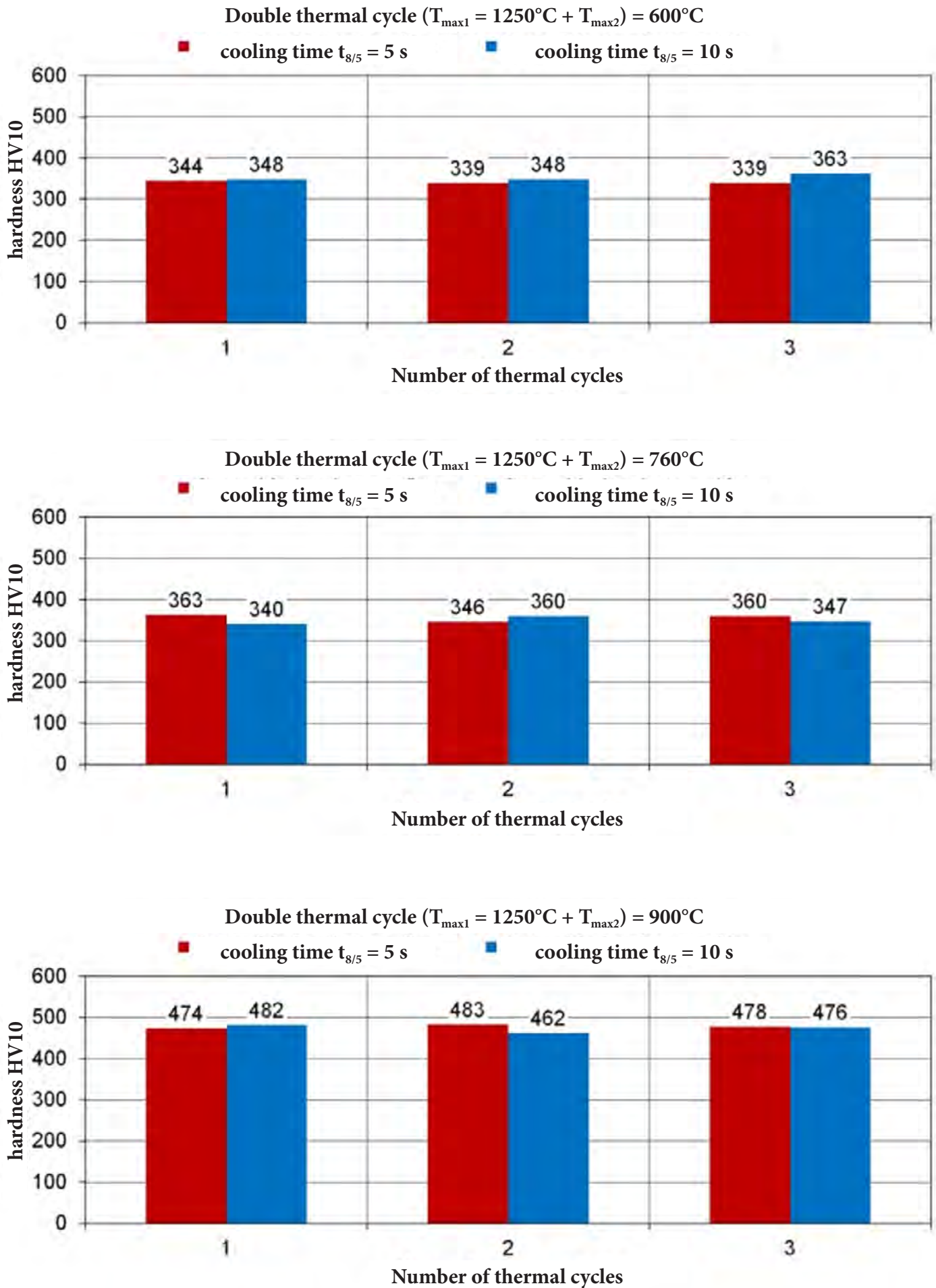


Fig. 17. Average values of hardness HV10 in relation to the simulated SWC areas of steel S1100QL in relation to cooling time $t_{8/5}$ = 5 s and 10 s in the function of the number of welding thermal cycles in relation to double thermal cycles: a) $T_{max1} = 1250^{\circ}\text{C} + T_{max2} = 600^{\circ}\text{C}$, b) $T_{max1} = 1250^{\circ}\text{C} + T_{max2} = 760^{\circ}\text{C}$ and c) $T_{max1} = 1250^{\circ}\text{C} + T_{max2} = 900^{\circ}\text{C}$

Discussion

The microstructure of the base material of steel S1300QL contained martensite having an average hardness of 486 HV_{10av}. (Fig. 2).

In terms of all of the variants related to the single thermal cycle, the microstructure of the simulated HAZ areas of steel S1300QL contained martensite characterised by average hardness restricted within the range of 433 HV_{10av}. to 487 HV_{10av}. (Fig. 3–5).

In relation to the double thermal cycle $T_{max1} = 1250^{\circ}\text{C} + T_{max2} = 600^{\circ}\text{C}$ and cooling time $t_{8/5} = 5$ s, the microstructure of the simulated HAZ areas contained the mixture of bainite and martensite characterised by average hardness restricted within the range of 339 HV_{10av}. to 344 HV_{10av}. (Fig. 6).

In relation to the double thermal cycle $T_{max1} = 1250^{\circ}\text{C} + T_{max2} = 600^{\circ}\text{C}$ and cooling time $t_{8/5} = 10$ s, the microstructure of the simulated HAZ areas contained the mixture of bainite, martensite and small amounts of ferrite characterised by average hardness restricted within the range of 348 HV_{10av}. to 363 HV_{10av}. (Fig. 7).

As regards all the repetitions of heating in relation to the double thermal cycle $T_{max1} = 1250^{\circ}\text{C} + T_{max2} = 760^{\circ}\text{C}$ and cooling times $t_{8/5} = 5$ and $t_{8/5} = 10$ s, the microstructure of the simulated HAZ areas contained the mixture of high-tempered martensite and small amounts of “fresh” martensite along grain boundaries characterised by average hardness restricted within the range of 340 HV_{10av}. to 363 HV_{10av}. (Fig. 8 and 9). The “fresh” martensite was formed from austenite (precipitated along grain boundaries) as a result of the exceeding of temperature AC_1 during the second thermal cycle. In relation to steel S1300QL, the value of temperature AC_1 amounted to 706°C .

As regards all the repetitions of heating in relation to the double thermal cycle ($T_{max1} = 1250^{\circ}\text{C} + T_{max2} = 900^{\circ}\text{C}$), the microstructure of the simulated HAZ areas contained the mixture of martensite and small amounts of ferrite (Fig. 10 and 11). In relation to cooling time

$t_{8/5} = 5$ s, the average hardness values were restricted within the range of 474 HV_{10av}. to 483 HV_{10av}. (Fig. 10). In turn, in relation to cooling time $t_{8/5} = 10$ s, the average hardness values were restricted within the range of 462 HV_{10av}. to 482 HV_{10av}. (Fig. 11).

According to data provided by the manufacturer of steel S1300QL (SSAB company), the minimum value of impact energy at a temperature of -40°C amounts to 27 J [1]. Because the thickness of the plate made of steel S1300QL amounted to 7 mm, the impact specimens used in the tests were thinner (5 mm x 10 mm x 55 mm). For the above-named specimens, the minimum impact energy should amount to 2/3 of the nominal KV, where $KV_{nominal} = 27$ J (in accordance with the guidelines of the Polish Register of Shipping) [14]. In view of the foregoing, the minimum impact energy of the specimens made of steel S1300QL, tested at a temperature of -40°C , should amount to 18 J.

In relation to single thermal cycles ($T_{max} = 1250^{\circ}\text{C}$) and double thermal cycles ($T_{max1} = 1250^{\circ}\text{C} + T_{max2} = 600^{\circ}\text{C}$ and $T_{max1} = 1250^{\circ}\text{C} + T_{max2} = 900^{\circ}\text{C}$), the test results regarding the average impact energy values concerning the simulated HAZ areas of steel S1300QL (presented in Figures 12, 13 and 15) revealed that all of the simulation variants (related a testing temperature of -40°C and that of $+20^{\circ}\text{C}$) satisfied the required criterion of 18 J.

In relation to the double thermal cycle $T_{max1} = 1250^{\circ}\text{C} + T_{max2} = 760^{\circ}\text{C}$ and both cooling times $t_{8/5}$, i.e. 5 s and 10 s, the impact energy of the simulated HAZ area of steel S1300QL failed to satisfy the minimum criterion $KV = 18$ J (Fig. 14).

The test results regarding the average impact energy values concerning the simulated HAZ areas of steel S1300QL in relation to the single thermal cycle ($T_{max} = 1250^{\circ}\text{C}$; Fig. 16) revealed that the lowest hardness value of 433 HV_{10av}. was obtained in relation to triple heating and cooling time $t_{8/5} = 10$ s. In turn, the highest hardness value of 487 HV_{10av}. was obtained

in relation to double heating and cooling time $t_{8/5} = 5$ s.

As regards the double thermal cycle ($T_{\max 1} = 1250^{\circ}\text{C} + T_{\max 2} = 600^{\circ}\text{C}$), the lowest hardness value of 339 HV_{10av}. was obtained in relation to double and triple heating and cooling time $t_{8/5} = 5$ s. In turn, the highest hardness value of 363 HV_{10av}. was obtained in relation to triple heating and cooling time $t_{8/5} = 10$ s (Fig. 17a).

As regards the double thermal cycle ($T_{\max 1} = 1250^{\circ}\text{C} + T_{\max 2} = 760^{\circ}\text{C}$), the lowest hardness value of 340 HV_{10av}. was obtained in relation to single heating and cooling time $t_{8/5} = 10$ s. In turn, the highest hardness value of 363 HV_{10av}. was obtained in relation to single heating and cooling time $t_{8/5} = 5$ s (Fig. 17b).

As regards the double thermal cycle ($T_{\max 1} = 1250^{\circ}\text{C} + T_{\max 2} = 900^{\circ}\text{C}$), the lowest hardness value of 462 HV_{10av}. was obtained in relation to double heating and cooling time $t_{8/5} = 10$ s. In turn, the highest hardness value of 483 HV_{10av}. was obtained in relation to double heating and cooling time $t_{8/5} = 5$ s (Fig. 17c).

The tests concerning the steel with the simulated HAZ revealed specific trends as regards changes in the microstructure of the steel and its mechanical properties (hardness and toughness). It is expected that steels such as S1300QL should be characterised by high strength, high yield point (in particular) as well as favourable toughness at lower temperature. The most favourable combination of high toughness and high hardness of the simulated HAZ of steel S1300QL was obtained using the double thermal cycle in relation maximum temperature $T_{\max 1} = 1250^{\circ}\text{C} + T_{\max 2} = 600^{\circ}\text{C}$, both cooling times, i.e. $t_{8/5} = 5$ s and 10 s and all repetitions of the heating process as well as the double thermal cycle $T_{\max 1} = 1250^{\circ}\text{C} + T_{\max 2} = 900^{\circ}\text{C}$ in relation to both cooling times, i.e. $t_{8/5} = 5$ s and 10 s and the number of the repetitions of the heating process restricted within the range of 1 to 3.

Conclusions

The above-presented tests and their results justified the formulation of the following conclusions:

1. Depending on the thermal cycle variants, the microstructure of the simulated HAZ area of steel S1300QL underwent changes of its structural composition, ranging from martensite in relation to the single thermal cycle, through the mixture of bainite and martensite in relation to the double cycle $T_{\max 1} = 1250^{\circ}\text{C} + T_{\max 2} = 600^{\circ}\text{C}$, the mixture of high-tempered martensite and "fresh" martensite along grain boundaries in relation to the double cycle $T_{\max 1} = 1250^{\circ}\text{C} + T_{\max 2} = 760^{\circ}\text{C}$ to the mixture of martensite and small amounts of ferrite in relation to the double cycle $T_{\max 1} = 1250^{\circ}\text{C} + T_{\max 2} = 900^{\circ}\text{C}$.
2. In relation to single ($T_{\max} = 1250^{\circ}\text{C}$) and double ($T_{\max 1} = 1250^{\circ}\text{C} + T_{\max 2} = 600^{\circ}\text{C}$ and $T_{\max 1} = 1250^{\circ}\text{C} + T_{\max 2} = 900^{\circ}\text{C}$) thermal cycles and all cooling times, the impact energy of the simulated HAZ area of steel S1300QL satisfied the minimum criterion $KV = 18$ J (related to thinner specimens) and was restricted within the range of 20 J to 54 J in relation to a testing temperature of -40°C and within the range of 36 J to 62 J in relation to a testing temperature $+20^{\circ}\text{C}$.
3. In relation to the double thermal cycle $T_{\max 1} = 1250^{\circ}\text{C} + T_{\max 2} = 760^{\circ}\text{C}$ and both cooling times $t_{8/5}$, i.e. 5 s and 10 s, the impact energy of the simulated HAZ area of steel S1300QL failed to satisfy the minimum criterion $KV = 18$ J and was restricted within the range of 11 J to 17 J in relation to a testing temperature of -40°C .
4. In terms of steel S1300QL, the number of the repetitions of the thermal cycle of preset parameters (between single and triple heating) did not trigger any clearly noticeable tendency as regards changes in the impact every values related to the simulated HAZ areas.
5. The recommended thermal cycle enabling the obtainment of the appropriate

combination of the high toughness and high hardness of the simulated HAZ areas of steel S1300QL (being similar to the hardness of the base material of the steel) was the double thermal cycle of the maximum temperature $T_{max1} = 1250^{\circ}\text{C} + T_{max2} = 600^{\circ}\text{C}$ in relation to both cooling times, i.e. $t_{8/5} = 5$ and 10 s and all repetitions of the heating process as well as the double thermal cycle $T_{max1} = 1250^{\circ}\text{C} + T_{max2} = 900^{\circ}\text{C}$ in relation to both cooling times, i.e. $t_{8/5} = 5$ s and 10 s and the number of the repetitions of the heating process restricted within the range of 1 to 3.

References

- [1] SSAB brochure: Data sheet 2020 Strenx 1300 2017-04-20.
- [2] Krasnowski K., Sędek P., Łomozik M., Kwieciński K., Jachym R.: Badania metodami mechaniki pęknięcia wytrzymałości zmęczeniowej połączeń spawanych nowoczesnej niskostopowej stali konstrukcyjnej o wysokiej wytrzymałości. Sprawozdanie z pracy badawczej nr Hb-96, Instytut Spawalnictwa, Gliwice 2015.
- [3] Amraeia M., Skrikoa T., Björka T., Zhao X-L.: Plastic strain characteristics of butt-welded ultra-high strength steel (UHSS). *Thin-Walled Structures*, 2016, t. 109, s. 227–241.
- [4] Węglowski M.St., Zeman M.: Spawalność stali WELDOX o granicy plastyczności 1300 MPa. Seminarium Instytutu Spawalnictwa pt. „Nowoczesne stale do pracy w ekstremalnych warunkach eksploatacyjnych”, 19. 04. 2012.
- [5] Holly S., Haslberger P., Zügner D., Schnitzer R., Kozeschnik E.: Development of high-strength welding consumables using calculations and microstructural characterisation. *Welding in the World*, 2018, vol. 62, pp. 451–458, <https://doi.org/10.1007/s40194-018-0562-1>.
- [6] Keehan E., Andrén O., Karlsson L., Muruganath M., Bhadeshia H.: Microstructural and mechanical effects of nickel and manganese on high strength weld metals. *Trends in Welding Research*, 2002, pp. 695–700.
- [7] Keehan E., Karlsson L., Andrén H.O.: Influence of carbon, manganese and nickel on microstructure and properties of strong steel weld metals: part 1 – effect of nickel content. *Science and Technology of Welding & Joining*, 2006, vol. 11, no. 1, pp. 1–8.
- [8] Keehan E., Karlsson L., Andrén H. O., Bhadeshia H.: Influence of carbon, manganese and nickel on microstructure and properties of strong steel weld metals: part 2 – impact toughness gain resulting from manganese reductions. *Science and Technology of Welding & Joining*, 2006, vol. 11, no. 1, pp. 9–18, <https://doi.org/10.1179/174329306X77849>.
- [9] Mięka J., Wojnar L.: Zastosowanie metod analitycznych w ocenie spawalności stali. Fotobit, Kraków 1996.
- [10] Zeman M.: Analiza stanu zagadnienia i ukierunkowanie badań wraz z praktycznymi przykładami zastosowań metod matematycznych w analizowanym zakresie. Praca badawcza Instytutu Spawalnictwa, Hc-60 (C-31.3.4), CPBR 7.3 „Techniki spawalnicze”, 1987.
- [11] PN-EN ISO 148-1:2017-02 Metale. Próba udarności sposobem Charpy'ego. Część 1: Metoda badania.
- [12] PN-EN ISO 17639:2013-12 Badania niszczące spawanych złączy metali. Badania makroskopowe i mikroskopowe złączy spawanych.
- [13] PN-EN ISO 6507-1:2018-05 Metale. Pomiar twardości sposobem Vickersa. Część 1: Metoda badania.
- [14] Polski Rejestr Statków. Przepisy klasyfikacji i budowy statków morskich. Część IX: Materiały i spawania. Lipiec, 2017.